International Journal of Structural Glass and Advanced Materials Research

Original Research Paper

Development of a Reliable Failure Assessment Diagram by Persian Curve

[1]Abdolrasoul Ranjbaran, [2]Mohammad Ranjbaran and [3]Fatema Ranjbaran

[1]Department of Civil and Environmental Engineering, Shiraz University, Shiraz, Iran
[2]Department of Chemical Engineering, Yasuj University, Yasuj, Iran
[3]Department of Mechanical Engineering, Shiraz University, Shiraz, Iran

Article history
Received: 26-01-2021
Revised: 08-03-2021
Accepted: 24-03-2021

Corresponding Author:
Abdolrasoul Ranjbaran
Department of Civil and Environmental Engineering, Shiraz University, Shiraz, Iran
Email: ranjbarn@shirazu.ac.ir

Abstract: A conventional tool for assessing the integrity of structures containing flaws is, the Failure Assessment Diagram (FAD). The (FAD) is a combination of the limiting conditions for load, the flaw size and fracture toughness or yielding stress. The abscissa is the load ratio and the ordinate is the toughness ratio. The toughness ratio is defined as a function of the load ratio. Three options are available for this function. The (FAD) drive is based on parameters of fracture mechanics. Classical fracture mechanics contains epistemic uncertainty and is unreliable. As a result, the state of the art for the (FAD) is also unreliable. The present authors' team, conducted an extensive investigation in the past two decades, which led to the birth of the change of state philosophy that is digested in the Persian Curve. In the present paper the Persian Curve is used for development of a reliable (FAD). The validity of the work is verified via concise mathematical logics and comparison of the results with those of the others.

Keywords: Failure Assessment Diagram, Change of State Philosophy, Persian Curve, State Functions, Uncertainty, Epistemic

Introduction

A conventional tool for assessing the integrity of structures containing flaws is, the Failure Assessment Diagram (FAD), a two-dimensional construct, which is a combination of the limiting conditions for load, the flaw size and fracture toughness or yielding stress. The abscissa is the load ratio and the ordinate is the toughness ratio. The toughness ratio is defined as a function of the load ratio. Three options are available for this function. The (FAD) drive is based on parameters of fracture mechanics. Classical fracture mechanics contains epistemic uncertainty and is unreliable. As a result, the state of the art for the (FAD) is also unreliable. Toward detection and removal of uncertainty the relevant literature briefly reviewed as follow.

A number of methods are available for assessing the integrity of structures containing flaws. Milne *et al*. (1988), selected one of the available methods and defined a route for establishing the integrity of a structure under consideration. Zhao (1989), developed a methodology for the reliability analysis of structural steel component with pre-existing cracks. The CEGB R6 is used for assessing the critical state of the structure. A rigorous methodology for the system reliability analysis of a jacket structure under both extreme wave and fatigue conditions, is presented by (Shetty, 1992). Bloom (1995) presented a brief history of the evolution of the CEGB R6 failure assessment diagram procedure used in assessing defects in structural components. The research into elastic-plastic crack tip field expanded using the first two terms of the Williams expansion to characterize the degree of crack tip constraint, by (MacLennan, 1996). Chell *et al*. (1999), prepared guidelines to address proof test issues and describe procedures, in the form of road map, for implementing state of the art fracture technology into the design and analysis of a proof test. The crack tip parameters T and Q were used to quantify the crack tip constraint in mode I, by (Ayatollahi, 1998). Welding residual stresses can, in combination with operating stresses, lead to premature failure of components by failure mechanisms such as fatigue cracking and fracture. It is therefore important that welding residual stresses are accounted for properly in safety assessment codes such as the Nuclear Electric code R6 and BS 7910. This is what is done by (May, 2002). Talei-Faz (2003) presented an investigation into

the performance of offshore tubular components containing large defects. The significance of the residual strength of cracked tubular members is considered with respect to inspection and maintenance of structural integrity. An investigation of structural monitoring is presented by (De Leeuw, 2004). Shabakhty (2004) research subject was durable reliability of jack-up platforms with the aim to explore the possibilities for the extension of the life-time. Sisan (2005), investigated the influence of prior thermal and mechanical loading on brittle and ductile fracture behavior. A three-dimensional-constraint based failure methodology based on failure assessment diagrams has been proposed using the analytical expression for constraint loss, by (Yusof, 2006). Dobmann *et al.* (2007), investigated new technologies for detection, classification and sizing of defects in combination with probabilistic (FAD) approaches. The fracture behavior of a hollow cylinder with internal circumferential crack under uniform tensile loading is examined by (Bach *et al*., 2009). Neto *et al.* (2008) investigated the structural integrity assessment of cracked piping of Pressurized Water Reactor nuclear reactors primary systems. An actual assessment has been carried out on cracked, circular hollow section, tubular K-joint containing a surface crack located at the crown location, using BS 7910:2005 (FAD) by (Lie and Yang, 2009). Ayala-Uraga (2009) considered the reliability-based assessment of deteriorating ship-shaped offshore structures. The aim of (Hosseini, 2010) study was to evaluate the effect of crack in corrosion defects on the failure pressure of natural gas transmission pipelines. Research on structural lifetime, reliability and risk analysis approaches for power plant components and systems was conducted by (Cronvall, 2011). The aim of (Elsaadany *et al*., 2012), was determination of shakedown boundary and fitness-assessment-diagrams for cracked pipe bends. Qu (2013) investigated the applicability of AIP579-1 PFSs (partial safety factor) and developed new PFSs which could provide enough accuracy for approximate evaluation of the safety margin. Hosseini *et al.* (2013), conducted experimental rupture tests to investigate the failure behavior of longitudinally oriented corrosion, crack and crack with corrosion. Ductile fracture and structural integrity of pipelines and risers was the subject of dissertation of (Kofiani, 2013). Hosseini (2014) considered crack in corrosion flaw assessment in thin-walled pipe. Fracture assessment of cracked components under biaxial loading is investigated by (Arafah, 2014). Vesga Rivera (2014) presented a combined engineering critical assessment which involved the examination of materials used to transport flue-gas and established a methodology to determine fracture toughness alongside with the (FAD) to assess the integrity of pipelines. The failure analysis and damage prevention on offshore pipelines under external loaded is studied by (Zhang, 2016). Sahu *et al.* (2015) worked on determination of fracture toughness curve using R-6 failure assessment method. Fracture assessments of large-scale straight pipes and elbows of various pipe diameters and crack sizes is reported by (Ainsworth *et al*., 2016). Orrock (2018) investigated the effects that scaling has on key structural integrity concepts, namely, stress fields, stress intensity factors and the J-integral. The influence of biaxial loading on the assessment of structures with defects is the subject of (Meek, 2017) study. Fuentes *et al.* (2018) provided a structural integrity assessment method for the analysis of non-metallic materials which uses BS 7910 Option 1 (FAD). Updating failure probability of a welded joint considering monitoring and inspection is investigated by (Mai, 2018). Hoh *et al.* (2018) worked on (FAD) analysis of fatigue test results for X65 welded joints. A study on the failure analysis of the neutron embrittled reactor pressure vessel support using finite element analysis is conducted by (Han, 2018). The title of (Sumesh and Arun Narayanan, 2018) paper is, influence of notch depth to width ratios on J-integral and critical failure load of single edge notched tensile aluminum 8011 alloy specimens. Coêlho *et al.* (2019) compared both British standard BS 7910 (2013) and American standard API 579/ASME FFS-1 (2016) stress intensity factor solutions by considering a series of semielliptical surface cracks located in the external surface of a pressurized hollow cylinder in the axial direction. Mechanical behavior of high strength structural steel under high loading rates is studied by (Alabi, 2019). Pillai *et al.* (2019) work covers the validation of standard safety assessment procedure in the new BS 7910: 2013+ A1:2015 for cracked joints. Analysis of crack behavior in pipeline system using (FAD) based on numerical simulation under XFEM is proposed by (Montassir *et al*., 2020).

The state of the art of the (FAD) contains epistemic uncertainty, that should be modified. The current authors research team detected the need for remedy and after extensive research (Ranjbaran, 2010; Ranjbaran *et al*., 2013; Ranjbaran and Ranjbaran, 2014; 2016; 2017; Ranjbaran *et al*., 2020a; 2020b; 2020c; 2020d; 2021; Amirian and Ranjbaran, 2019; Baharvand and Ranjbaran, 2020), in the last two decades, proposed the Change of State Philosophy (CSP) which digested in the Persian Curves (PC) (Ranjbaran *et al*., 2020a), that is used for the development of a reliable (FAD). The validity of the work is verified via concise mathematical logics and comparison of the results with those of the others as follows.

Basic Formulation

The analysis of a phenomenon, considered as a change in the state of the system, is conducted as follows. A decreasing parameter for the system, called stiffness and the inverse of stiffness, called flexibility are considered. The contributing parameters, as shown in Fig. 1, are defined as, the system stiffness at a changed state ($k_{SS} = k_S$-k_C), the system stiffness at intact state (k_S), the change stiffness (k_C), the system flexibility at the changed state ($f_{SS} = f_S$+f_C), the system flexibility at intact state (f_S) and the change flexibility (f_C). The (CSP) formulation is commenced with the obvious relation between the system parameters, as shown in Fig. 2 and defined in Eq. (1):

$$\left(k_{SS} = \frac{1}{f_{SS}}\right) \times \left(\frac{1}{k_S} = f_S\right) \Rightarrow \left(\frac{k_{SS}}{k_S} = \frac{f_S}{f_{SS}}\right) \tag{1}$$

Equation (1) is rearranged to obtain the (k_{SS}) and (k_C), in Eq. (2):

$$\begin{aligned} k_{SS} &= \frac{f_S \times k_S}{f_S + f_C} = \frac{f_S}{f_S + f_C} \times k_S = S_R \times k_S \\ k_C &= \frac{f_C \times k_S}{f_S + f_C} = \frac{f_C}{f_S + f_C} \times k_S = F_R \times k_S \end{aligned} \tag{2}$$

in which the phenomenon functions (collection of the failure function (F_R) and the survive function (S_R)) are defined in Eq. (3):

$$F_R = \frac{f_C}{f_S + f_C} \in [0,1] S_R = \frac{f_S}{f_S + f_C} \in [0,1] \tag{3}$$

Definition of the dimensionless phenomenon functions in a unit interval, introduced a down to earth method for human knowledge. Since obvious concepts are used, then the proposed method is free of epistemic uncertainty and the common problems in the conventional methods, such as singularity, instability and etc. Consequently, the authors decided to complete the work. To continue, the unknown parameters in Eq. (4) should be explicitly determined:

$$k_C = ?\ f_C = ? \tag{4}$$

The investigation for explicit definition of the aforementioned functions, is continued in the next paragraph via definition and construction of the so called, state functions.

Development of a functional (F_R and S_R) in terms of two functions (f_S and f_C) is not possible. Therefore, the phenomenon functions are customized for ($k_S = f_S = 1$) to define the destination function (D) and the origin function (O), which are collectively called the state functions and the state ratio (R) in Eq. (5). This is an artifice to define functions (D and O) in terms of only one variable (R):

$$F_R \Rightarrow D \quad S_R \Rightarrow O \quad f_C \Rightarrow R \tag{5}$$

Consequently the (D) and (O) are defined in terms of the (R) in Eq. (6):

$$D = \frac{R}{1+R} \quad O = \frac{1}{1+R} \quad R = \frac{D}{R} \tag{6}$$

The state functions may be considered as solution of the boundary value problems in Eq. (7), in which (min) and (max) denote minimum and maximum respectively:

$$D = \begin{cases} \min = 0 & @R = 0 \\ \max = 1 & @R = \infty \end{cases} \quad O = \begin{cases} \max = 1 & @R = 0 \\ \min = 0 & @R = \infty \end{cases} \tag{7}$$

The (R) with one end in the infinity, as shown in Fig. 3, is not a good working parameter. Moreover, this ratio is itself a function, so it is not wise to be used as an independent variable. Therefor, the state variable ($\xi \in [0, 1]$) with a zero value ($\xi = 0$) at the origin and a unit value ($\xi = 1$) at the destination is defined. The state variable is the phenomenon's abstract lifetime. In terms of the state variable, the boundary value problems in Eq. (7) is rewritten in Eq. (8):

$$D = \begin{cases} \min = 0 & @\xi = 0 \\ \max = 1 & @\xi = 1 \end{cases} \quad O = \begin{cases} \max = 1 & @\xi = 0 \\ \min = 0 & @\xi = 1 \end{cases} \tag{8}$$

Investigation for construction of solution for boundary value problems in Eq. (8), led the authors to use their experience in structural mechanics, finite element method, mathematics and extensive research (Ranjbaran *et al*., 2020a). The results are the state functions defined in Eq. (9) and shown in Fig. 4:

$$\begin{aligned} D &= 0.25\left(2 - 1 + 6\xi^2 - 4\xi^3 - \cos(\pi\xi)\right) \\ O &= 0.25\left(2 + 1 - 6\xi^2 + 4\xi^3 + \cos(\pi\xi)\right) \end{aligned} \tag{9}$$

Equation (9) is an average of polynomial and trigonometric functions as defined in Eq. (10):

$$\begin{aligned} D &= 0.25\left(0 + 6\xi^2 - 4\xi^3\right) + 0.25\left(1 - \cos\pi\xi\right) \\ O &= 0.25\left(2 - 6\xi^2 + 4\xi^3\right) + 0.25\left(1 + \cos\pi\xi\right) \end{aligned} \tag{10}$$

The authors invite the readers from all over the world to propose new (better in some sense) state functions in place of Eq. (9).

Now attention is paid to construction of the phenomenon functions. Via the definition of the (k_{SS}) and the (f_{SS}) and the crack compliance (f_C) in fracture mechanics (Anderson, 2005), the authors detected a fact that, the (f_C) is directly proportional to the (k_S)! This detection is called "the Persian Principle of Change (PPC)". In view of this principle the (f_C) is defined in Eq. (11):

$$f_C/R = k_S/1 \rightarrow f_C = k_S R \rightarrow f_C = k_S\, D/O \tag{11}$$

Note that Eq. (11) is an alternative for the whole fracture mechanics (Anderson, 2005)! Insertion of Eq. (11) into Eq. (3) concluded in the general definition for the phenomenon functions in Eq. (12):

$$F_R = \frac{k_S^2 D}{O + k_S^2 D} S_R = \frac{O}{O + k_S^2 D} \tag{12}$$

The (k_S) is not explicitly known so it is not a feasible working parameter. Toward better definition and preparation for using reliable data, Eq. (12) is rewritten in Eq. (13) in terms of the positive control parameters (a_M) and (b) (Ranjbaran *et al*., 2020a). The flexibility for translation and rotation of phenomenon functions in the (1×1) working box, which lets the experts to enforce their will, is provided by selection of two control parameters from calibration of reliable data:

$$F_R = \frac{a_M D^b}{O^b + a_M D^b} S_R = \frac{O^b}{O^b + a_M D^b} \tag{13}$$

To this end the proposed formulation is mathematically in abstract form. Consequently, it is a certain universal formulation, in a sense that it is independent of geometry, coordinates, material properties, size and changing agent. Therefore, it equally applies to all natural-phenomena.

Persian Curve

As observed, the proposed formulation is derived based on logical reasoning and concise mathematics, without a need for construction of differential and integral equations, which is the paramount basis of the conventional methods of analysis in human knowledge. Consequently, the proposed formulation is reliable and free of epistemic uncertainty, because it is based on obvious and certain basis, for example the definition of flexibility as inverse of stiffness in Eq. (1).

To prepare for determination of control parameters for a phenomenon, the (F_R) is renamed as Persian-Fasa-curve (P_F), the (S_R) is renamed as Persian-Shiraz-curve (P_S) and the two collectively called the Persian curve (P_C), defined in Eq. (14), in which (P_O) is the ordinate of the origin point (O) and (P_T) is the ordinate of the truncated (end) point (T). Note that insertion of (P_O = 1 and P_T = 0) and (P_O = 0 and P_T = 1) into Eq. (14) conclude into (F_R) and (S_R) respectively as in Eq. (13):

$$P_C = \left(P_O O^b + P_T a_M D^b\right) \Big/ \left(O^b + a_M D^b\right) \tag{14}$$

In comply with the vocabulary of human knowledge, the (P_S) is the unified equation for capacity and reliability representing a decreasing data and the (P_F) is the unified equation for the probability and fragility representing an increasing data. Moreover, in comply with the common practice in stochastic analysis the (probability) density distribution, here called the Persian-Zahedan-curve (P_Z) and defined as the derivative of phenomenon functions with respect to the (ξ). The (P_Z) is casted in Eq. (15), in which ($D^{(1)}$) is derivatives of (D) with respect to (ξ). In spite of the paramount role of the density distribution in stochastic theory, it has no such important role in the (CSP) and it is used only for comparison with the conventional one:

$$F_R = \int_0^{\xi} P_Z dx \quad S_R = \int_{\xi}^{1} P_Z dx \quad P_Z = \frac{b a_M D^{b-1} O^{b-1} D^{(1)}}{\left(O^b + a_M D^b\right)^2} \tag{15}$$

In order to determine the control parameters, Eq. (14) is rearranged as in Eq. (16):

$$a_M = a_C \Big/ \left(D/O\right)^b \quad a_C = \left(P_C - P_O\right) \Big/ \left(P_T - P_C\right) \tag{16}$$

Equation (16), in terms of control parameters (a_M and b) is nonlinear. An artifice is used, for their simple computation, as follows. It is noted, in view of the definition of the state functions in Eq. (9), that at the Middle point (M) (D_M/O_M = 1). Substitution of (D_M/O_M = 1) into Eq. (16) led into an explicit definition for (a_M). Then the coordinate of the Next point (N) is used, in Eq. (16), to determine (b). The results are expressed in terms of the key Points (KPS) ordinates in Eq. (17). This equation, equally applies, to both of increasing and decreasing data as shown in Fig. 5:

$$a_C = \frac{P_C - P_O}{P_T - P_C}, C = N \,\&\, M \; b = \frac{Log\left(a_N/a_M\right)}{Log\left(D_N/O_N\right)} \tag{17}$$

The Key Points (KPS) are defined as the Origin point (O), the Middle point (M), the end point (T) and the Next point (N) (a point between the other three), in Eq. (18) and shown in Fig. 5 for both of decreasing and increasing data:

$$O\left(0.0, P_O\right) \;\; N\left(\xi_N, P_N\right) \;\; M\left(0.5, P_M\right) \;\; T\left(1.0, P_T\right) \tag{18}$$

DOI: 10.3844/sgamrsp.2021.68.81

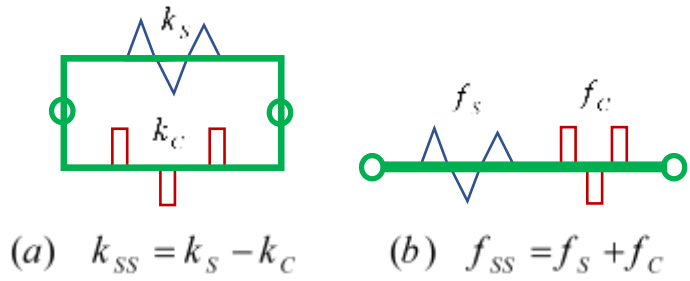

Fig. 1: Spring models for conventional analyses

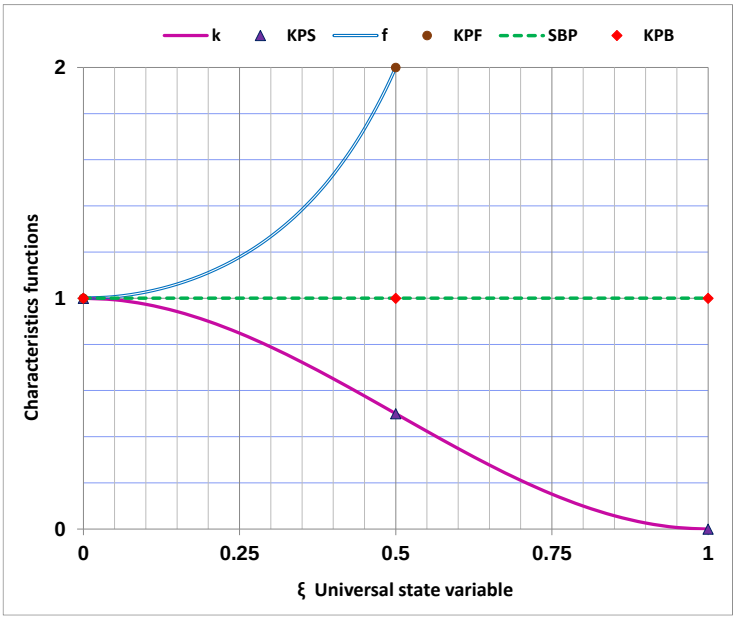

Fig. 2: Change of state philosophy basic equations

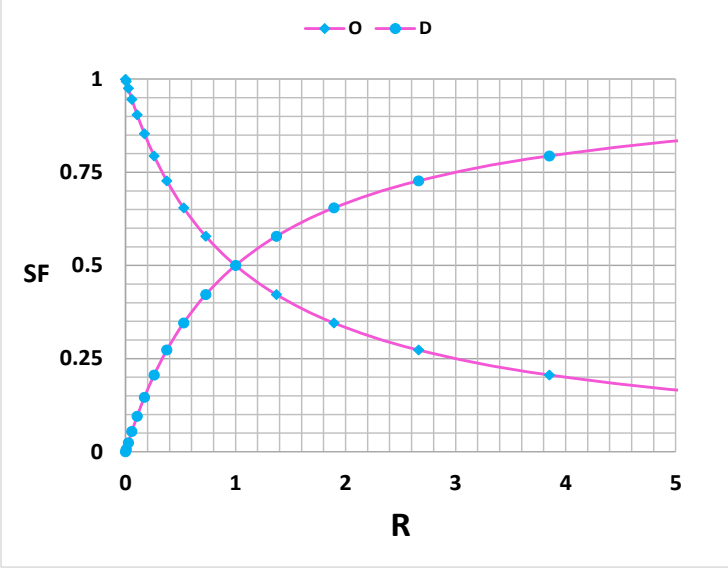

Fig. 3: State functions versus state ratio

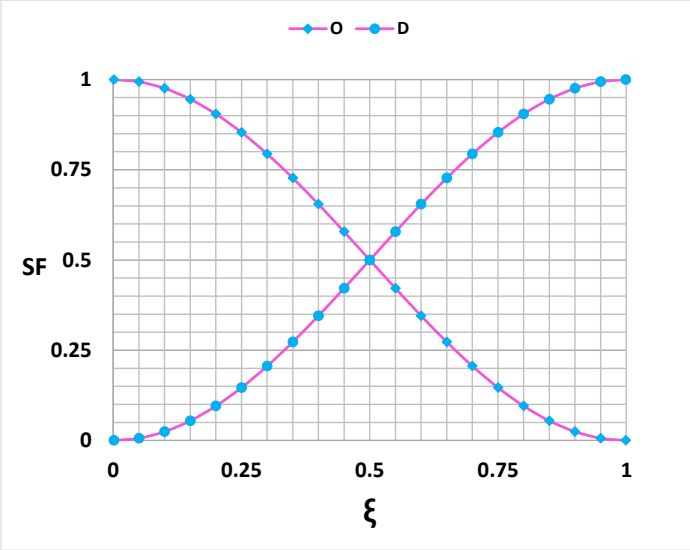

Fig. 4: State functions versus state variable

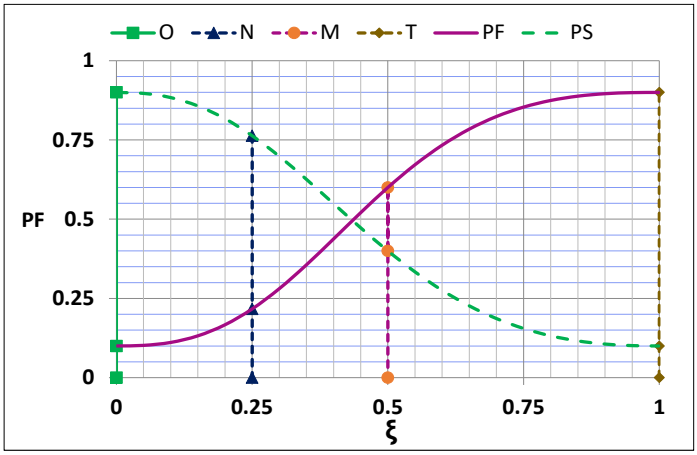

Fig. 5: Key points on Persian curves

Unified Persian Curve

Close investigation of the reliable capacity data in the literature (Ranjbaran *et al*., 2020a), concluded into the key points, on the lower bound of capacity, in Eq. (19):

$$O(0.0,1.0)\quad N(0.25,\ 0.86)\quad M(0.5,\ 0.4)\quad T(1.0,\ 0.1) \tag{19}$$

Insertion of Eq. (19) into Eq. (17) concluded into the control parameters, in Eq. (20):

$$a_M = 2.0\ \ b = 1.0 \tag{20}$$

Substitution of control parameters in Eq. (20) into Eq. (14) and Eq. (15) concluded in the unified capacity function (*PSU*), unified fragility function (*PFU*) and unified density function (*PZU*), in Eq. (21):

$$P_{SU} = \frac{1-0.8D}{1+D} P_{FU} = \frac{1.8D}{1+D} P_{ZU} = \frac{2D^{(1)}}{(1+D)^2} \tag{21}$$

Failure Assessment Diagram

Persian curve is defined in terms of an abstract life time called state variable in a unit interval ($\xi \in [0, 1]$). In real phenomena, the lifetime (λ) is selected in a truncated interval ($\lambda \in [\lambda_O, \lambda_T]$), where ($\lambda_O$) is the lifetime origin and (λ_T) is the lifetime destination. Lifetime is a characteristic of the system. In common practice the ratio (to make it user friendly) of a predefined parameter (F_Y) and an intentionally defined one (F_E) is expressed as lifetime (λ), as in Eq. (22):

$$\lambda^2 = F_Y \ / \ F_E \tag{22}$$

For the case of steel structural systems (F_Y) is the yield stress, (F_E) is the Euler's stress and lifetime (λ) is the relative slenderness ratio, as in Eq. (23). The other parameters are (L_e) effective length, (r) is radius of gyration, (E) is initial modulus:

$$\lambda^2 = \left(F_Y\right) \Big/ \left(\frac{\pi^2 E}{L_e^2/r^2}\right) = \frac{F_Y}{\pi^2 E} \times \frac{L^2}{r^2} \tag{23}$$

For systems containing flaw the lifetime (λ) is denoted by (L_r or S_r). In order to use the Persian Curve, the lifetime (λ) should be mapped on the state variable (ξ), as in Eq. (24):

$$\xi = \left(\lambda - \lambda_O\right) / \left(\lambda_T - \lambda_O\right) \quad \lambda = \left(1-\xi\right)\lambda_O + \xi\lambda_T \tag{24}$$

The key points ordinates on unified Persian curves are defined in Eq. (25). The values recorded in Eq. (25) are the corresponding parameters for (O, N, M and T) which are computed from Eq. (21) and (24) for completeness:

PC	O	N	M	T
λ	0.000	0.750	1.500	3.000
ξ	0.000	0.250	0.500	1.000
P_{FU}	0.000	0.237	0.600	0.900
P_{SU}	1.000	0.763	0.400	0.100
P_{ZU}	0.000	1.686	1.364	0.000

(25)

Formulation is complete now. The work is verified in the following section.

Verification

To this end, it is shown that the Persian Curve is a reliable tool for analysis of failure phenomena, conceived as a change in the structural system. Concise mathematical formulation presented in previous sections. In comply with the literature, the validity of the work is verified via comparison of the results with those of the others in the following examples.

Example 1

Compare the Unified Persian curve with the (FAD) defined in Eq. (26):

$$K_r = \left(1 - 0.1L_r^2 + 0.1L_r^4\right) / \left(1 + 3L_r^4\right) \tag{26}$$

Solution

The (FAD) from Eq. (26) (KI) (Milne *et al*., 1988) is compared with the unified Persian curve (PSU) in Fig. 6. Based on the reliability of Persian curve the modified (FAD) (KIM) is defined in Eq. (27) and shown in Fig. 6. The lifetime is mapped onto the state variable as ($L_r = 2.25\ \xi$):

$$K_r^M = \left(1 - 0.1L_r^2 + 0.1L_r^4\right) / \left(1 + L_r^4\right) \tag{27}$$

Note that the modified (FAD) goes through the unified Key Points (KPU). A set of test data (TEST) (Gibstein and Moe, 1986) is also shown. Comparison of results shown that the conventional results contain uncertainty and should be replaced by Persian curve.

Example 2

The Unified Persian curve is compared with the (FAD) defined in Eq. (28):

$$K_r = \left(1 - 0.14L_r^2\right)\left(0.3 + 0.7\exp\left(-0.65L_r^6\right)\right) \tag{28}$$

Solution

The unified Persian curve (PSU) is compared with the (FAD) from Eq. (28) (KII) (Zhao, 1989; Shetty, 1992; MacLennan, 1996; Talei-Faz, 2003; Shabakhty, 2004; Yusof, 2006; Bach *et al*., 2009; Lie and Yang, 2009; Hosseini, 2010; Schaser, 1994; Hosseini, 2014; Arafah, 2014; Vesga Rivera, 2014; Sahu *et al*., 2015; Akbar and Setiawan, 2016; Coêlho *et al*., 2019; Dai *et al*., 2020; Irfaee, 2019; Pillai *et al*. 2019) in Fig. 7. The lifetime is mapped onto the state variable as ($L_r = 2.25\ \xi$). On the same figure, a set of test data (TEST) by (Gibstein and Moe, 1986) is also shown. The (KII) goes through the unified key points, but over estimates the test results, therefore contain uncertainty and is not reliable.

Example 3

Compare the Unified Persian curve with the (FAD) defined in Eq. (29):

$$K_r = \left(1 + 0.5L_r^2\right)^{-1/2}\left(0.3 + 0.7\exp\left(-0.65L_r^6\right)\right) \tag{29}$$

Solution

The (FAD) from Eq. (29) (KIII) by (Ocejo *et al*., 1997; Ainsworth, 1993; May, 2002; MacLennan, 1996; Schaser, 1994; Sanderson *et al*., 2015; Ainsworth *et al*., 2016; Amann, 2017; Orrock, 2018; Meek, 2017; Amara *et al*., 2018; Fuentes *et al*., 2018; Hassani *et al*., 2018; Hoh *et al*., 2018; Mai, 2018; Montassir *et al*., 2020) is compared with the unified Persian curve (PSU) in Fig. 8. The lifetime is mapped onto the state variable as ($L_r = 2.25\ \xi$). A set of Test data (TEST) by (Gibstein and Moe, 1986) is also shown. The (KIII) goes through the unified key points. But over estimation of the test

results, is conceived as a sign for presence of uncertainty and unreliability of the conventional (FAD) in Eq. (29).

Example 4

A conventional (FAD) is defined in Eq. (30). Compare the Unified Persian curve with the conventional (FAD):

$$K_r = \left(1 - 0.02L_r^2\right)\left(0.35 + 0.7\exp\left(-1.4L_r^6\right)\right) \tag{30}$$

Solution

The (FAD) from Eq. (30) (KIV) by (Ainsworth *et al*., 1999; Dai *et al*., 2020) and the test data (TEST) by (Gibstein and Moe, 1986) are compared with the unified Persian curve (PSU) in Fig. 9. The lifetime is mapped onto the state variable as (L_r = 2.25 ξ). The (KIV) goes through the unified key points, but over estimates the test results, therefore contain uncertainty and is not reliable.

Example 5

Compare the Unified Persian curve with the (FAD) defined in Eq. (31):

$$K_r = S_r\left(\frac{8}{\pi^2}Ln\sec\left(\frac{\pi S_r}{2}\right)\right)^{-1/2} \tag{31}$$

Solution

The (FAD) from Eq. (31) (KBR) (Bloom, 1995; Schaser, 1994; de Oliveira Dias, 2014; Arafah, 2014) is compared with the unified Persian curve (PSU) in Fig. 10. The lifetime is mapped onto the state variable as (S_r = ξ). A set of test data (TEST) (Gibstein and Moe, 1986) is also shown. The (KBR) overestimates the test data and the (PSU) so is unreliable.

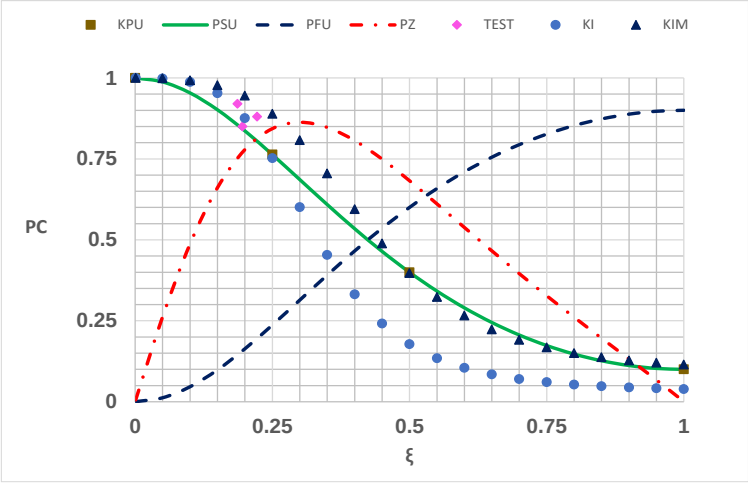

Fig. 6: Compare PC with FAD (KI)

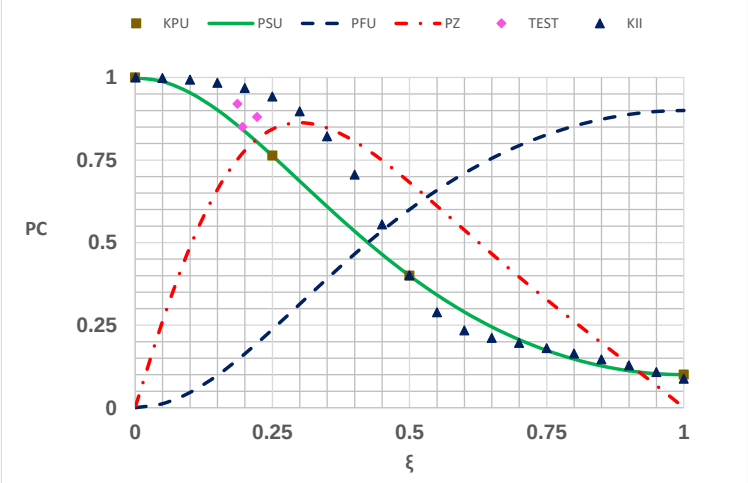

Fig. 7: Compare PC with FAD (KII)

DOI: 10.3844/sgamrsp.2021.68.81

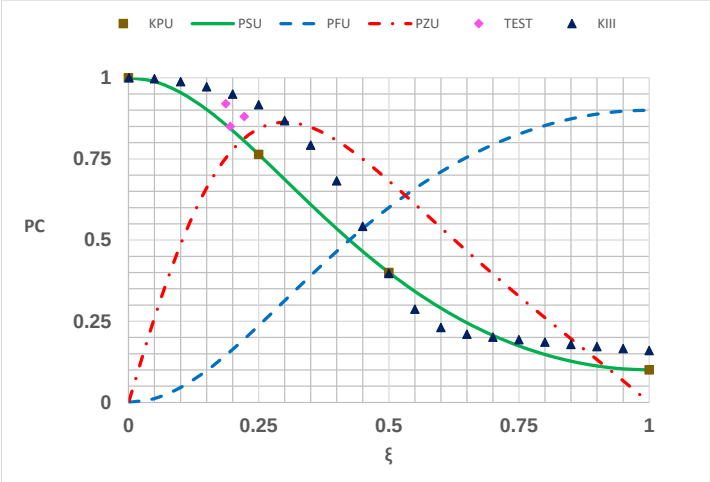

Fig. 8: Compare PC with FAD (KIII)

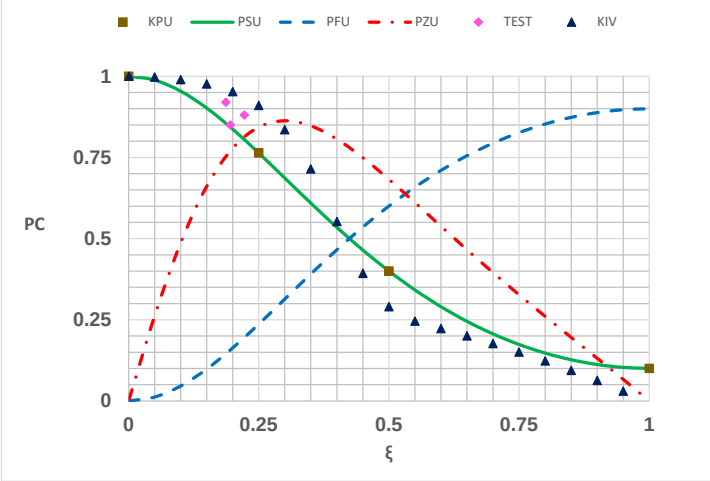

Fig. 9: Compare PC with FAD (KIV)

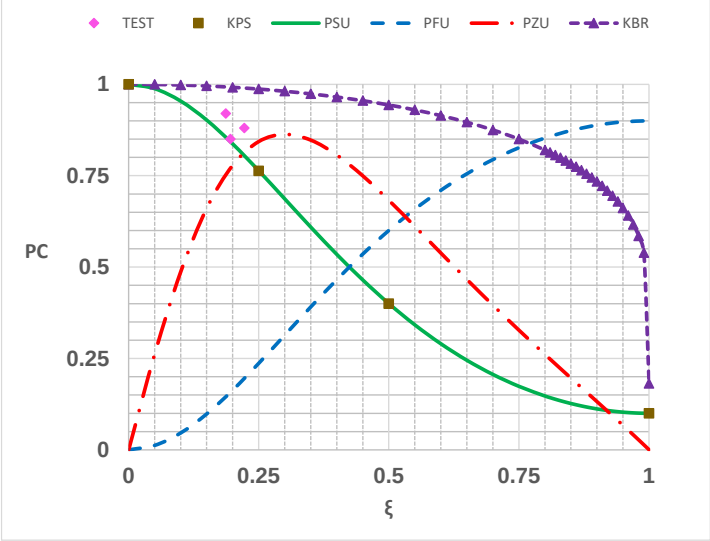

Fig. 10: Compare PC with FAD (KBR)

Discussion

The conventional (FAD) is based on conventional fracture mechanics, which is based on singularity of stress at crack tip. Stress singularity at crack tip is a wrong concept, then the conventional fracture mechanics and the (FAD) contain epistemic uncertainty and are not reliable. On the other hand, the proposed formulation is logical and reliable. The parameter (L_r) is defined as the ratio of the applied stress over the yield stress. The applied stress is not a property of the system. Therefore, only the yield stress is considered as the effective parameter for the system. Experience in determination of ultimate strength of structures shown that the yield stress is not enough. But the geometry also should be considered. For example, for two columns with the same cross section and yield stress, the capacity of the longer one is less than the other! The combination of the material and geometric properties, in the form of the relative slenderness ratio (λ), as in Eq. (23), is the necessary and sufficient condition. Note that, Eq. (23) is the inverse of the current definition of (L_r) when applied stress is selected as the Euler's stress. Consequently, replacement of the (L_r) with the (λ) is recommended.

Conclusion

The following conclusion obtained from this study. The failure phenomenon is conceived as the change of state of the system. Based on logical reasoning and concise mathematics, the change of state is expressed in terms of the Persian curve. The Persian curve is completely calibrated from four key points on real world data. Making use of reliable data in the literature, the unified control parameters and the unified Persian curves are explicitly expressed in term of the state variable. The unified Persian-Shiraz curve (PSU) is proposed as a reliable (FAD). Validity of the work is verified via concise mathematical logics and comparison of the results with those of the others in five examples. The proposed formulation is recommended to be used as a certain logical basis for the assessment codes of practice such as BS7910 and API 579. Based on its logical basis, there is no restriction on the application of the proposed method. What remains, is to determine the modified slenderness ratio and section capacity for structures with defect.

Acknowledgement

Thanks to all members of our family, specially Zahra, who provided a calm state and condition, at the time of Corona at home and encouraged writing of the paper. Note that the names of Persian curves were selected as the names of cities, Fasa, Shiraz and Zahedan in Iran, where the authors birthed, grown, educated and worked.

Author's Contributions

All authors equally contributed in this study.

Ethics

This article is original and contains unpublished material. The corresponding author confirms that all of the other authors have read and approved the manuscript and no ethical issues involved with declaration of no conflict of interest.

References

Ainsworth, R. A. (1993). The use of a failure assessment diagram for initiation and propagation of defects at high temperatures. Fatigue & Fracture of Engineering Materials & Structures, 16(10), 1091-1108. https://doi.org/10.1111/j.1460-2695.1993.tb00080.x

Ainsworth, R. A., Gintalas, M., Sahu, M. K., Chattopadhyay, J., & Dutta, B. K. (2016). Application of failure assessment diagram methods to cracked straight pipes and elbows. International Journal of Pressure Vessels and Piping, 148, 26-35. https://www.sciencedirect.com/science/article/abs/pii/S0308016116303660

Ainsworth, R. A., Hooton, D. G., & Green, D. (1999). Failure assessment diagrams for high temperature defect assessment. Engineering Fracture Mechanics, 62(1), 95-109. https://www.sciencedirect.com/science/article/abs/pii/S0013794498000873

Alabi, A. A. (2019). Mechanical behaviour of high strength structural steel under high loading rates (Doctoral dissertation, Brunel University London). https://bura.brunel.ac.uk/handle/2438/19430

Amirian, P., & Ranjbaran, A. (2019). Studying the Effect of Fundamental Structural Period on the Seismic Fragility Curves of Two-Span Integral Concrete Box Girder Bridges. Iranian Journal of Science and Technology, Transactions of Civil Engineering, 44(1), 11-26. https://link.springer.com/article/10.1007/s40996-019-00312-9

Arafah, D. Z. R. (2014). Fracture assessment of cracked components under biaxial loading. https://www.politesi.polimi.it/handle/10589/92881

Ayala-Uraga, E. (2009). Reliability-based Assessment of Deteriorating Ship-shaped Offshore Structures. https://ntnuopen.ntnu.no/ntnu-xmlui/handle/11250/237683

Ayatollahi, M. R. (1998). Geometry and constraint effects in mixed mode fracture (Doctoral dissertation, University of Bristol). https://ethos.bl.uk/OrderDetails.do?uin=uk.bl.ethos.265450

Anderson, T. L. (2005). Fracture mechanics: fundamentals and applications. Taylor and Francis Group LLC, USA, 2005. https://books.google.com.pk/books/about/Fracture_Mechanics.html?id=MxrtsC-ZooQC&redir_esc=y

Akbar, M., & Setiawan, R. (2016). Failure assessment diagram constraint used for integrity analysis of cylindrical shell with crack. Journal of Ocean, Mechanical and Aerospace Science and Engineering, 27; 18-25. http://citeseerx.ist.psu.edu/viewdoc/download?doi=10.1.1.742.2286&rep=rep1&type=pdf

Amann, C. (2017). Probabilistic fracture mechanics of forged rotor disks. https://publikationen.bibliothek.kit.edu/1000071647

Amara, M., Bouledroua, O., Meliani, M. H., Muthanna, B. G. N., Abbas, M. T. and Pluvinage, G. (2018). Assessment of pipe for CO2 transportation using a constraint modified CTOD failure assessment diagram. Structural Integrity and Life, 18(2); 149-153.

Bach, M., Wang, X., & Bell, R. (2009, January). Constraint-Based Fracture Mechanics Analysis of Cylinders With Circumferential Cracks. In International Conference on Offshore Mechanics and Arctic Engineering (Vol. 43468, pp. 83-89). https://asmedigitalcollection.asme.org/OMAE/proceedings-abstract/OMAE2009/83/337972

Baharvand, A., & Ranjbaran, A. (2020). Seismic Fragility Functions Grounded on State-Based Philosophy: Application to Low to Midrise Steel Frame Buildings. KSCE Journal of Civil Engineering, 24(6), 1787-1798. https://link.springer.com/article/10.1007/s12205-020-0350-5

Bloom, J. M. (1995). Deformation plasticity failure assessment diagram (DPFAD) for materials with non-Ramberg-Osgood stress-strain curves. https://asmedigitalcollection.asme.org/pressurevesseltech/article-abstract/117/4/346/438625

Chell, G. G., McClung, R. C., Russell, D. A., Garr, K., & Donnelly, B. (1999). Guidelines for proof test analysis. Marshall Space Flight Center, National Aeronautics and Space Administration. https://core.ac.uk/download/pdf/42767836.pdf

Coêlho, G. D. C., Silva, A. A., Santos, M. A., Lima, A. G., & Santos, N. C. (2019). Stress intensity factor of semielliptical surface crack in internally pressurized hollow cylinder—a comparison between BS 7910 and API 579/ASME FFS-1 solutions. Materials, 12(7), 1042. https://www.mdpi.com/1996-1944/12/7/1042

Cronvall, O. (2011). Structural lifetime, reliability and risk analysis approaches for power plant components and systems. VTT. https://www.vttresearch.com/sites/default/files/pdf/publications/2011/P775.pdf

De Leeuw, B. (2004). Analysis and assessment of structural integrity monitoring. University of London, University College London (United Kingdom). https://search.proquest.com/openview/df9f6bd1bac3223391918f23a76f91e0/1?pq-origsite=gscholar&cbl=2026366&diss=y

Dobmann, G., Boulavinov, A., Kyöning, M., & Kurz, J. (2007). Quantitative NDE-New Technologies for Detection, Classification and Sizing of Defects in Combination with Probabilistic Fad-Approaches. https://repository.lib.ncsu.edu/bitstream/handle/1840.20/31375/O02_1.pdf?sequence=1

Dai, Y., Liu, Y., Qin, F., Chao, Y. J., & Chen, H. (2020). Constraint modified time dependent failure assessment diagram (TDFAD) based on C (t)-A2 (t) theory for creep crack. International Journal of Mechanical Sciences, 165, 105193. https://www.sciencedirect.com/science/article/abs/pii/S0020740319312470

de Oliveira Dias, H. F. B. (2014). Failure Assessment on Effects of Pressure Cycle Induced Fatigue on Natural Gas Pipelines. https://pdfs.semanticscholar.org/1567/321fce87b48446589db5baef1ee2fc330971.pdf

ElSaadany, M. S., Younan, M. Y., & Abdalla, H. F. (2012, July). Determination of shakedown boundary and fitness-assessment-diagrams of cracked pipe bends. In Pressure Vessels and Piping Conference (Vol. 55089, pp. 61-70). American Society of Mechanical Engineers. https://asmedigitalcollection.asme.org/PVP/proceedings-abstract/PVP2012/61/281482

Fuentes, J. D., Cicero, S., Ibáñez-Gutiérrez, F. T., & Procopio, I. (2018). On the use of British standard 7910 option 1 failure assessment diagram to non-metallic materials. Fatigue & Fracture of Engineering Materials & Structures, 41(1), 146-158. https://doi.org/10.1111/ffe.12668

Gibstein, M., & Moe, E. T. (1986). Brittle fracture in tubular joints. In International offshore mechanics and arctic engineering. Symposium. 5 (pp. 144-152). https://pascal-francis.inist.fr/vibad/index.php?action=getRecordDetail&idt=7962308

Han, G. (2018). A study on the failure analysis of the neutron embrittled reactor pressure vessel support using finite element analysis (Doctoral dissertation, Purdue University).

Hoh, H. J., Pang, J. H. L., & Tsang, K. S. (2018). Failure Assessment Diagram (FAD) analysis of fatigue test results for X65 welded joints. In MATEC Web of Conferences (Vol. 165, p. 21011). EDP Sciences. https://www.matec-conferences.org/articles/matecconf/abs/2018/24/matecconf_fatigue2018_21011/matecconf_fatigue2018_21011.html

Hosseini, A., Cronin, D., & Plumtree, A. (2013). Crack in corrosion defect assessment in transmission pipelines. Journal of Pressure Vessel Technology, 135(2). https://asmedigitalcollection.asme.org/pressurevesseltech/article-abstract/135/2/021701/378330/Crack-in-Corrosion-Defect-Assessment-in?redirectedFrom=fulltext

Hosseini, S. A. (2010). Assessment of crack in corrosion defects in natural gas transmission pipelines. MSc Thesis, Department of Mechanical Engineering, University of Waterloo, Ontario, Canada. https://uwspace.uwaterloo.ca/bitstream/handle/10012/5099/Hosseini_Seyed%20Aliakbar.pdf?sequence=1

Hosseini, S. A. (2014). Crack in Corrosion Flaw Assessment in Thin-Walled Pipe. https://uwspace.uwaterloo.ca/handle/10012/8734

Hassani, M., Bouledroua, O., Meliani, M. H., Sadou, L., & Pluvinage, G. (2018). Assessment of a cracked pipe subject to transient flow by the Monte Carlo method. Pipeline Science and Technology, 2(2), 135-145.

Irfaee, M. M. (2019). Effect of mixed-mode loading on fatigue and fracture assessment of a steel twin box-girder bridge (Doctoral dissertation, Colorado State University). https://mountainscholar.org/handle/10217/195407

Kofiani, K. N. (2013). Ductile fracture and structural integrity of pipelines & risers (Doctoral dissertation, Massachusetts Institute of Technology). https://dspace.mit.edu/handle/1721.1/79292

Lie, S. T., & Yang, Z. M. (2009). BS7910: 2005 failure assessment diagram (FAD) on cracked circular hollow section (CHS) welded joints. Advance Steel Construe, 5(4), 406e20. https://citeseerx.ist.psu.edu/viewdoc/download?doi=10.1.1.1079.1470&rep=rep1&type=pdf

MacLennan, I. J. (1996). Two parameter engineering fracture mechanics (Doctoral dissertation, University of Glasgow). http://theses.gla.ac.uk/6756/1/1996MacLennanPhd.pdf

Mai, A. Q. (2018). Updating Failure Probability of a Welded Joint Considering Monitoring and Inspection-For Offshore Wind Turbine Substructures (Doctoral dissertation, Université de Liège, Liège, Belgique). https://orbi.uliege.be/handle/2268/230027

May, P. S. (2002). The effect of welding residual stresses on the fracture resistance of ductile steels. file:///C:/Users/IT%20Department/Downloads/Philip_Stewart_May-2002-PhD-Thesis.pdf

Meek, C. (2017). The Influence of Biaxial Loading on the Assessment of Structures with Defects. The University of Manchester (United Kingdom). https://search.proquest.com/openview/1504b78870d9fb290df33131726a9469/1?pq-origsite=gscholar&cbl=51922&diss=y

Milne, I., Ainsworth, R. A., Dowling, A. R., & Stewart, A. T. (1988). Assessment of the integrity of structures containing defects. International Journal of Pressure Vessels and Piping, 32(1-4), 3-104. https://www.sciencedirect.com/science/article/abs/pii/0308016188900713

Montassir, S., Yakoubi, K., Moustabchir, H., Elkhalfi, A., Rajak, D. K., & Pruncu, C. I. (2020). Analysis of Crack Behaviour in Pipeline System Using FAD Diagram Based on Numerical Simulation under XFEM. Applied Sciences, 10(17), 6129. https://www.mdpi.com/2076-3417/10/17/6129

Neto, M. M., Cruz, J. R. B., & de Jong, R. P. (2008). On the structural integrity assessment of cracked piping of PWR nuclear reactors primary systems. Progress in nuclear energy, 50(7), 800-817. https://www.sciencedirect.com/science/article/abs/pii/S0149197007000765

Ocejo, J.R., Gutierrez-Solana F. and Gorrochategui I (1997). Failure assessment diagram. Report/SINTAP/UC/05. University Cantabria, Spain.

Orrock, P. (2018). An Investigation Into the Effects of Scaling on Structural Integrity Assessments (Doctoral dissertation, University of Bristol). https://research-information.bris.ac.uk/ws/portalfiles/portal/174948210/Final_Copy_2018_05_08_Orrock_P_PhD.pdf

Pillai, V. S., Kolios, A., & Lie, S. T. (2019). Failure assessment of cracked uni-planar square hollow section T-, Y-and K-joints using the new BS 7910: 2013+ A1: 2015. Archive of Applied Mechanics, 89(5), 835-845. https://link.springer.com/article/10.1007/s00419-018-1423-5

Qu, Q. (2013). Development of fitness for service assessment method based on reliability. MSc Thesis, Sakai-Izumi Laboratory, University of Tokyo, Japan.

Ranjbaran, A., Ranjbaran, M., & Ranjbaran, F. (2020a). Change of State Philosophy & Persian Curves: The Final Destination of Human Knowledge. LAP LAMBERT Academic Publishing. ISBN: 978-620-2-68228-2

Ranjbaran, A., Ranjbaran, M., & Ranjbaran, F. (2020b). Building probability functions by Persian curves. International Journal of Structural Glass and Advanced Materials Research, 4(1); 225-232. https://doi.org/10.3844/sgamrsp.2020.225.232

Ranjbaran, M., & Ranjbaran, F. (2020c). A reliable fracture mechanics. International Journal of Reliability, Risk and Safety: Theory and Application, 3(1), 1-15. https://doi.org/10.30699/IJRRS.3.1.1

Ranjbaran, A., Ranjbaran, M., & Ranjbaran, F. (2020d). A reliable method of analysis for geotechnical data. International Journal of Structural Glass and Advanced Materials Research, 4(1); 276-293. https://doi.org/10.3844/sgamrsp.2020.276.293

Ranjbaran, A., Ranjbaran, M., & Ranjbaran, F. (2021). Building design rule for glass structures by Persian curve. International Journal of Structural Glass and Advanced Materials Research, 5(1): 1-13. https://doi.org/10.3844/sgamrsp.2021.1.13

Ranjbaran, A. (2010). Analysis of cracked members the governing equations and exact solutions. https://www.sid.ir/en/Journal/ViewPaper.aspx?ID=196258

Ranjbaran, A., & Ranjbaran, M. (2014). New finite-element formulation for buckling analysis of cracked structures. Journal of Engineering Mechanics, 140(5), 04014014. https://ascelibrary.org/doi/abs/10.1061/(ASCE)EM.1943-7889.0000734

Ranjbaran, A., & Ranjbaran, M. (2016). State functions: the milestone of fracture. Archive of Applied Mechanics, 86(7), 1311-1324. https://link.springer.com/article/10.1007/s00419-015-1115-3

Ranjbaran, A., & Ranjbaran, M. (2017). Innovative theory for the compliance computation in rotors. Scientia Iranica, 24(4), 1779-1788. http://scientiairanica.sharif.edu/article_4269.html

Ranjbaran, A., Rousta, H., Ranjbaran, M. O., Ranjbaran, M. A., Hashemi, M., & Moravej, M. T. (2013). A necessary modification for the finite element analysis of cracked members detection, construction and justification. Archive of Applied Mechanics, 83(7), 1087-1096. https://link.springer.com/article/10.1007/s00419-013-0736-7

Sahu, M. K., Chattopadhyay, J., & Dutta, B. K. (2015). Determination of fracture toughness curve using R-6 method. https://repository.lib.ncsu.edu/bitstream/handle/1840.20/33878/SMiRT-23_Paper_679.pdf?sequence=1

Shabakhty, N. (2004). Durable reliability of jack-up platforms: The impact of fatigue, fracture and effect of extreme environmental loads on the structural reliability.

Shetty, N. (1992). System reliability of fixed offshore structures under fatigue deterioration. file:///C:/Users/IT%20Department/Downloads/Navilkumar_Shetty-1992-PhD-Thesis.pdf

Sisan, A. M. (2005). The influence of prior thermal and mechanical loading on fracture (Doctoral dissertation, University of Bristol). https://ethos.bl.uk/OrderDetails.do?uin=uk.bl.ethos.424411

Sumesh, C. S., & Arun Narayanan, P. J. (2018). Influence of Notch Depth-to-Width Ratios on J-Integral and Critical Failure Load of Single-Edge Notched Tensile Aluminium 8011 Alloy Specimens. Journal of Solid Mechanics, 10(1), 86-97. http://jsm.iau-arak.ac.ir/article_539695.html

Schaser, M. S. (1994). Material specific load combination factors for option 2 FAD curves. MSc thesis, Department of Civil Engineering, Cleveland State University, USA. https://engagedscholarship.csuohio.edu/cgi/viewcontent.cgi?article=1821&context=etdarchive

Talei-Faz, B. (2003). Fatigue and fracture of tubulars containing large cracks (Doctoral dissertation, UCL (University College London)). https://discovery.ucl.ac.uk/id/eprint/10102385/

Vesga Rivera, W. (2014). An evaluation of the structural integrity of HSLA steels exposed in simulated flue-gases under dynamic conditions for anthropogenic CO_2 transport. https://dspace.lib.cranfield.ac.uk/handle/1826/9652

Yusof, F. (2006). Three-dimensional constraint based fracture mechanics (Doctoral dissertation, University of Glasgow). http://theses.gla.ac.uk/70997/

Zhang, Y. (2016). Failure analysis and damage prevention on offshore pipelines under extreme loadings. PhD Dissertation, Interdisciplinary Graduate School, Nanyang Technological University, Singapore. file:///C:/Users/IT%20Department/Downloads/Thesis-ZHANG%20Yanmei.pdf

Zhao, W. (1989). Reliability analysis of fatigue and fracture under random loading. file:///C:/Users/IT%20Department/Downloads/Wangwen_Zhao-1989-PhD-Thesis.pdf

List of Symbols

a_M:	Control parameter at M
a_N:	Control parameter at N
b:	Control parameter (power)
CSP:	Change of State Philosophy
D:	Destination function
E:	Initial modulus
F:	Force
FAD:	Failure assessment diagram
F_y:	Yield limit
f_S:	System flexibility
f_C:	Change flexibility
F_S:	Dimensioned flexibility
fSS:	Survived flexibility
F_R:	Failure function
(F_R and S_R):	Phenomenon functions
f_W:	Weibull probability density function
F_W:	Weibull cumulative distribution function
γ:	Recovery rate
K_r:	Toughness ratio
k_S:	System stiffness
k_C:	Change stiffness

k_{SS}: Survived stiffness
KPF: Key points on Failure curve
KPS: Key points on Survive curve
KPS: Key points
KPU: Key points on unified Persian curves
L: Effective length
L/*r*: Slenderness ratio
L_r: Load ratio
LB: Lower bound
λ: Lifetime parameter
$\lambda = \frac{L}{r}\sqrt{\frac{F_y}{\pi^2 E}}$: Relative slenderness rati
λ_O: Lifetime origin
λ_T: Lifetime termination (end)
M: Middle point
N: Next point
O: Origin (start) point
O: Origin function
PC: Persian curve (s)
P_O: Origin point ordinate
P_N: Next point ordinate
P_M: Middle point ordinate
P_T: End point ordinate
P_{FU}: Unified Persian-failure function
P_{SU}: Unified Persian-survive function
P_{ZU}: Unified Persian-distribution function
P_Z: Persian-Distribution function
P_F: Persian-Failure function
P_S: Persian-survive function
P_C = (P_F and P_S): Persian curves
r: Effective radius of gyration
R: State ratio
S_r: Load ratio
S_R: Survive function
S_F = (*D* and *O*): State functions
T: Termination (end) point
UB: Upper bound
ξ: State variable
ψ: Displacement